COMPDYN 2015
5th ECCOMAS Thematic Conference on
Computational Methods in Structural Dynamics and Earthquake Engineering
M. Papadrakakis, V. Papadopoulos, V. Plevris (eds.)
Crete Island, Greece, 25–27 May 2015

SEISMIC ANALYSIS OF COUPLED BUILDINGS WITH MR DAMPER

Fangshu Lin[1], **Xilin Lu**[1]

[1] College of Civil Engineering, Tongji University
1239 Siping Road, Shanghai 200092, China
e-mail: fangshulin16@gmail.com, lxlst@tongji.edu.cn

Keywords: Coupled Building System, MR Damper, Structural Control Strategy, Seismic analysis.

Abstract. *The coupled building system has shown to be a viable approach to mitigate dynamic responses. In the system two adjacent buildings are connected together using coupling links such as magnetorheological (MR) dampers to work as a group. Therefore the forces can be transferred upon one another and eventually reduce critical responses. The coupled building systems have been successfully implemented for newly built buildings and used as a solution to retrofit existing buildings.*

The focus of this study is to comprehensively investigate the effectiveness of coupled building system interconnected by a MR damper considering both linear and nonlinear cases. The multistory benchmark SAC structures are selected as the adjacent buildings. Through numerical study, the control performance of different semi-active control strategies for MR damper are compared and evaluated. Furthermore, the robustness of different control strategies for pre-earthquake and post-earthquake cases is discussed. Finally, the cases of nonlinear adjacent buildings represented by hysteretic Bouc Wen models connected by MR damper are examined. The results show that using MR damper as the coupling link is an effective way to reduce the responses of both of the adjacent buildings under earthquake input. Some general conclusions and recommendations are also given for further research.

1 INTRODUCTION

The interconnecting of two adjacent buildings with dampers is an effective method to reduce dynamic responses. In recent years, various approaches of the coupled building system have been examined and applied to civil engineering structures [1-3]. In coupled building system, it is promising to use semi-active control device such as the magnetorheological (MR) damper as the coupled link. MR damper offers the adaptability similar to active control device with very small power sources. When utilizing the MR damper with complex nonlinear behavior in structural control, one of the challenges to achieve high levels performance is the selection and design of appropriate control algorithms based on the available feedback measurements.

The focus of this study is to comprehensively examine the efficacy of coupled building system interconnected by a MR damper under different control algorithms for both linear and nonlinear cases. Several control methods are implemented here including passive control and three semi-active controllers, i.e. clipped optimal controller, Lyapunov controller and pseudo-negative stiffness (PNS) controller. Through numerical study, the pros and cons of each control strategy for MR damper are discussed and evaluated. Furthermore the robustness of different control strategies for pre-earthquake and post-earthquake cases is discussed. The effectiveness of the coupled building system for seismic response mitigation is demonstrated in this study.

2 COUPLED BUILDING SYSTEM

2.1 Coupled building model

The adjacent buildings of 3 and 9 stories used in this study were designed based on the benchmark SAC structures which meet the seismic code and may represent typical low- and medium-rise buildings in Los Angeles, California region. Here the structures are simplified as two shear buildings. The two buildings are connected at the 3rd story with a MR damper. The story height of both building is 3.96 m. The mass and stiffness of each floor for building 1 are 4.945×10^5 kg and 1.72×10^8 N/m. For building 2, the mass and stiffness are 4.785×10^5 kg and 1.16×10^8 N/m. Damping in each mode is assumed to be 2% for both buildings. The first natural frequencies of two buildings are 0.49 Hz and 1.10 Hz.

The equation of motion of the coupled building system is

$$\mathbf{M}\ddot{\mathbf{x}} + \mathbf{C}\dot{\mathbf{x}} + \mathbf{K}\mathbf{x} = -\mathbf{M}\boldsymbol{\Gamma}\ddot{x}_g + \boldsymbol{\Lambda}f \tag{1}$$

where **M**, **C** and **K** are the mass, damping and stiffness matrices of the coupled system. $\boldsymbol{\Gamma}$ and $\boldsymbol{\Lambda}$ are the influence vectors considering ground motion and damper location, respectively. f is the feedback force of MR damper. **x** is the relative displacement vector. $\ddot{x}_g$ is the ground acceleration. The **M**, **C** and **K** matrices are defined as

$$\mathbf{M} = \begin{bmatrix} [\mathbf{M_1}]_{9\times9} & [\mathbf{0}]_{9\times3} \\ [\mathbf{0}]_{3\times9} & [\mathbf{M_2}]_{3\times3} \end{bmatrix}; \mathbf{C} = \begin{bmatrix} [\mathbf{C_1}]_{9\times9} & [\mathbf{0}]_{9\times3} \\ [\mathbf{0}]_{3\times9} & [\mathbf{C_2}]_{3\times3} \end{bmatrix}; \mathbf{K} = \begin{bmatrix} [\mathbf{K_1}]_{9\times9} & [\mathbf{0}]_{9\times3} \\ [\mathbf{0}]_{3\times9} & [\mathbf{K_2}]_{3\times3} \end{bmatrix} \tag{2}$$

The state-space expression of the equation of motion is

$$\dot{\mathbf{z}} = \mathbf{A}\mathbf{z} + \mathbf{B}\mathbf{u} \tag{3}$$

$$\mathbf{z} = \begin{bmatrix} \mathbf{x} \\ \dot{\mathbf{x}} \end{bmatrix}; \mathbf{u} = \begin{bmatrix} \ddot{x}_g \\ f \end{bmatrix} \tag{4}$$

$$\mathbf{A} = \begin{bmatrix} \mathbf{0} & \mathbf{I} \\ -\mathbf{M^{-1}K} & -\mathbf{M^{-1}C} \end{bmatrix}; \mathbf{B} = \begin{bmatrix} \mathbf{0} & \mathbf{0} \\ -\boldsymbol{\Gamma} & \mathbf{M^{-1}}\boldsymbol{\Lambda} \end{bmatrix} \tag{5}$$

where **z** is the state vector defined as displacement and velocity at lumped mass locations.

In this study, in order to illustrate the performance of nonlinear multi-story adjacent buildings connected by a MR damper, additional analyses are conducted. Here the hysteretic Bouc Wen models are selected to represent the nonlinearity of the structure in each floor. In this model, the ratio of the post yielding stiffness and elastic stiffness is selected to be 0.035.

2.2 MR damper model

In this study, a phenomenological Bouc-Wen model developed by Spencer et al. [4] is used to simulate the MR damper. The parameters of the Bouc-Wen model are given in Table 1 which is physically identified to represent a RD-8041-1 MR damper (LORD Corporation). The damper can generate specified peak to peak force higher than 550 lb (2447 N) due to a velocity input of 1.97 in/sec (5 cm/sec) with 1 Amp current level.

α_a	13.71 lb/in	α_b	41.99 lb/in-V	c_{0a}	3.72 lb-s/in
c_{0b}	5.96 lb-s/in-V	c_{1a}	14.91 lb-s/in	c_{1b}	102.68 lb-s/in-V
k_0	11.08 lb/in	k_1	0.01 lb/in	γ	23.44 in^{-2}
β	23.44 in^{-2}	A	155.32	x_0	0.00 in
n	2	η	60.00 s^{-1}		

Table 1: Parameters for the MR damper model.

2.3 Semi-active control strategies

One of the advantages of MR damper is that by semi-active control, the damper can effectively mitigate the responses as active control device while requiring very small power sources. Here in this study, five control strategies are implemented and evaluated. Note that in the implementation of all the algorithms, the available feedback measurements are the absolute acceleration of both buildings and control force. The other states are estimated using Kalman filter.

Passive on control (PON)

The first control method considered is passive on control, where the command voltage to the MR damper is held at a constant level of 2.8 V.

Clipped optimal control (COC1 and COC2)

The second and third are clipped optimal control, proposed by Dyke et al. [5]. First the LQG/H2 strategy is applied in calculating the optimal control force. The voltage input of MR damper is then determined using the following control law.

$$v = V_{max} H\{(f_d - f_m) f_m\} \tag{6}$$

where H{·} is the Heaviside step function, V_{max} is the maximum voltage to the current driver considering the saturation of the magnetic field in the MR damper.

Here two clipped optimal controllers COC1 and COC2 are designed which focus on minimizing the displacements and accelerations of both buildings, respectively. The maximum voltage applied is set to 2.8 V. For the design of COC1 and COC2, equal weight is selected for every floor and **R** is selected to be an identity matrix of proper order. A family of controllers can be designed by varying the weighting matrix **Q**. Here the **Q** matrix is determined based on the performance of these controllers in simulations by trial and error. For COC1 and COC2, the **Q** matrix weights are chosen to be 1.61×10^{15} and 1.78×10^{12} respectively.

Lyapunov stability-based control

Leitmann [6] applied Lyapunov's direct approach for the design of a semi-active controller. In this approach, Lyapunov fuction is selected as

$$V(\mathbf{z}) = \frac{1}{2}\|\mathbf{z}\|_P{}^2 \tag{7}$$

where $\|\mathbf{z}\|_P$ is defined by

$$\|\mathbf{z}\|_P = [\mathbf{z}^T\mathbf{P}\mathbf{z}]^{1/2} \tag{8}$$

and **P** is a real, symmetric, positive definite matrix. For a linear system, to ensure $\dot{V}$ is negative definite, the matrix **P** is determined using the Lyapunov equation below for a positive definite matrix $\mathbf{Q}_P$.

$$\mathbf{A}^T\mathbf{P} + \mathbf{P}\mathbf{A} = -\mathbf{Q}_P \tag{9}$$

The derivative of the Lyapunov fuction is

$$\dot{V} = -\frac{1}{2}\mathbf{z}^T\mathbf{Q}_P\mathbf{z} + \mathbf{z}^T\mathbf{P}\mathbf{B}\mathbf{f} + \mathbf{z}^T\mathbf{P}\mathbf{E}\ddot{x}_g \tag{10}$$

The only term that can be directly affected by a change in the control current is the middle term that contains the force vector **f**. Thus, the input to the damper which will minimize $\dot{V}$ is

$$v_i = V_{max}H((-\mathbf{z})^T\mathbf{P}\mathbf{B}_i f_i) \tag{11}$$

where H{·} is the Heaviside step function and f_i is the measured force of the *i*th damper.

In the controller design for this study, the positive definite matrix $\mathbf{Q}_P$ are selected arbitrarily based on the simulation results by trial and error.

Pseudo-negative stiffness (PNS) control

The PNS control method was first proposed by Iemura et al. [7, 8]. Here in this study, the PNS method is applied to MR damper with the input voltage changes depending on the movement direction [9]. The input voltage follows the solid line when the direction of motion is positive (from left to right) and follows the dashed line when the direction is negative (from right to left), shown in Figure 1. The control law expression is given by

$$v(x, \dot{x}) = -\text{sgn}(\dot{x}) \times S \times x + v_m \tag{12}$$

where *S* is the slope of the line, v_m is the input voltage at the central position, and *x* is the stroke of the damper. In this study, *S* and v_m are selected to be 4 V/in and 1.4 V respectively.

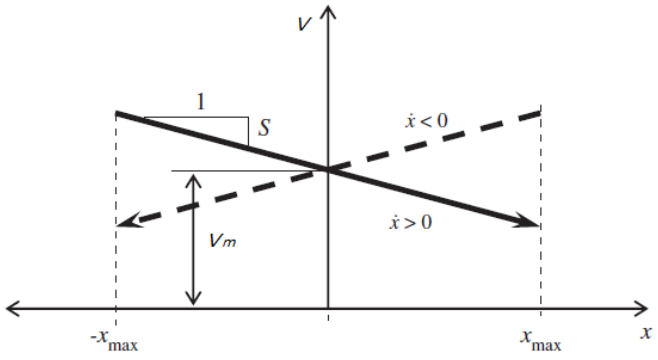

Figure 1: input voltage of PNS controller.

3 SIMULATION RESULTS

To evaluate the control performance of coupled building system with MR damper, numerical simulation is performed using different control strategies under El Centro earthquake input

in MATLAB/SIMULINK environment for both linear and nonlinear cases. PGA of the earthquake record is scaled to DBE (design basis earthquake) level for linear cases and MCE (maximum considered earthquake) level for nonlinear cases using the methods provided by relevant provisions with regards to the recommendations for earthquakes in California area [10]. Since the MR damper model used in this study is of lab scale, to achieve the required control capacity, the output force of the MR damper is multiplied by 4800 and the displacement is scaled such that 1 mm in the MR damper corresponds to 20 mm in the coupled building system. The sampling frequency is 4096 Hz.

The responses of both buildings and the control forces are selected as the evaluation criteria as shown in Table 2.

Peak Floor Displacement $J_1 = \max_{EQ}\left\{\frac{\max_{t,i}\lvert x_i(t)\rvert}{x^{max}}\right\}$	Normed Floor Displacement $J_5 = \max_{EQ}\left\{\frac{\max_{i}\lVert x_i(t)\rVert}{\lVert x^{max}\rVert}\right\}$	Control Force $J_9 = max_{EQ}\left\{\frac{\max_{t}\lvert f(t)\rvert}{W}\right\}$
Peak Interstory Drift $J_2 = \max_{EQ}\left\{\frac{\max_{t,i}\left(\frac{\lvert d_i(t)\rvert}{h_i}\right)}{d_n^{max}}\right\}$	Normed Interstory Drift $J_6 = max_{EQ}\left\{\frac{\max_{i}\left(\frac{\lVert d_i(t)\rVert}{h_i}\right)}{\lVert d_n^{max}\rVert}\right\}$	Peak Control Force $J_{10} = max_{EQ}\left\{\max_{t}\lvert f(t)\rvert\right\}$
Peak Floor Acceleration $J_3 = \max_{EQ}\left\{\frac{\max_{t,i}\lvert \ddot{x}_{ai}(t)\rvert}{\ddot{x}_a^{max}}\right\}$	Normed Floor Acceleration $J_7 = \max_{EQ}\left\{\frac{\max_{i}\lVert \ddot{x}_{ai}(t)\rVert}{\lVert \ddot{x}_a^{max}\rVert}\right\}$	RMS Control Force $J_{11} = max_{EQ}\{\lvert f_{RMS}(t)\rvert\}$
Peak Base Shear $J_4 = \max_{EQ}\left\{\frac{\max_{t}\lvert\sum_{i=1}^{\eta} m_i \ddot{x}_{a\eta_i}(t)\rvert}{F_b^{max}}\right\}$	Normed Base Shear $J_8 = \max_{EQ}\left\{\frac{\lVert\sum_{i=1}^{\eta} m_i \ddot{x}_{a\eta_i}(t)\rVert}{\lVert F_b^{max}\rVert}\right\}$	

Table 2: Summary of evaluation criteria.

3.1 Control performance assessment (linear)

First, the numerical simulation is conducted using a linear model of coupled building system interconnected by a MR damper. The evaluation results of the control performance under El Centro earthquake using the proposed criteria are listed and compared in Tables 3 and 4. As an example, the uncontrolled and COC2 controlled time histories of the top floor responses for both buildings are given in Figure 2. The performance of different control strategies considering the RMS responses over the height of the adjacent buildings is compared in Figure 3.

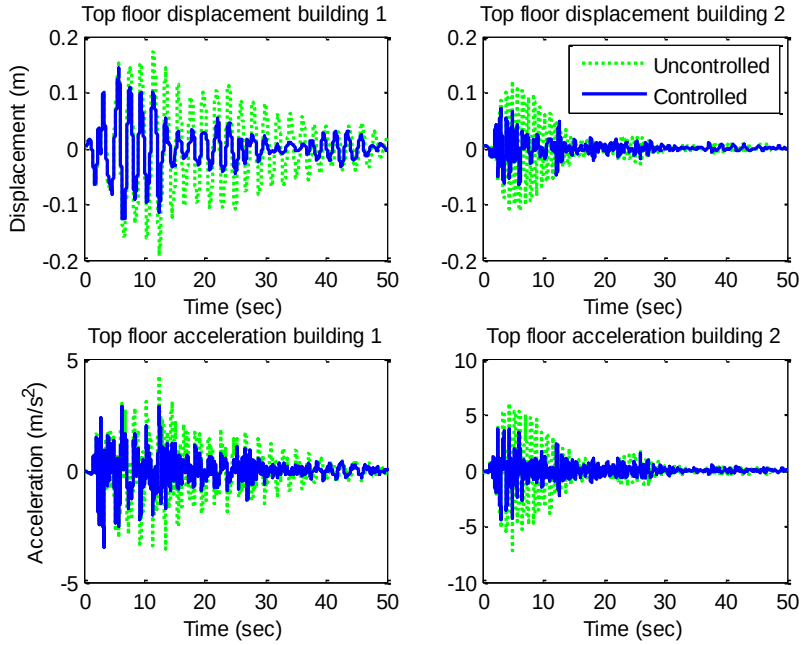

Figure 2: Time histories of top floor responses under COC2 control.

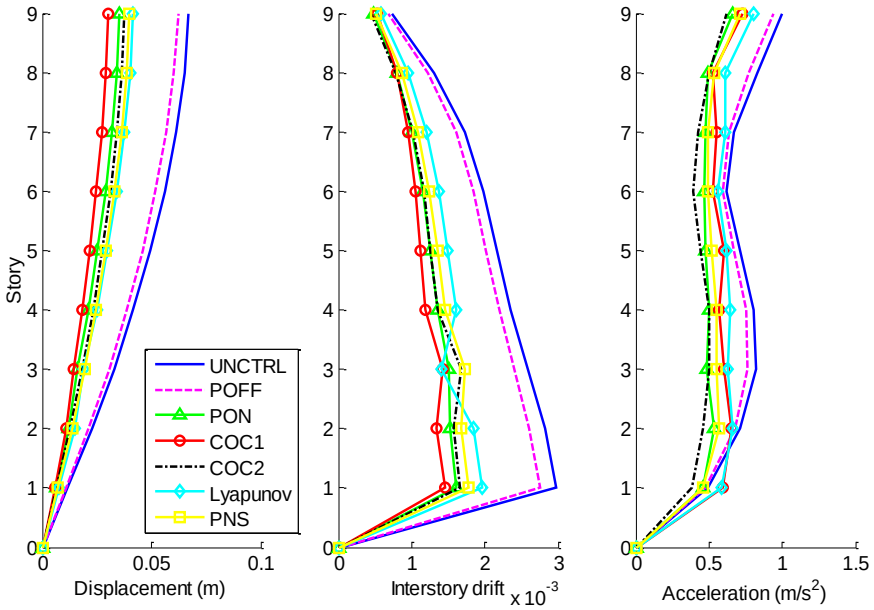

(a)

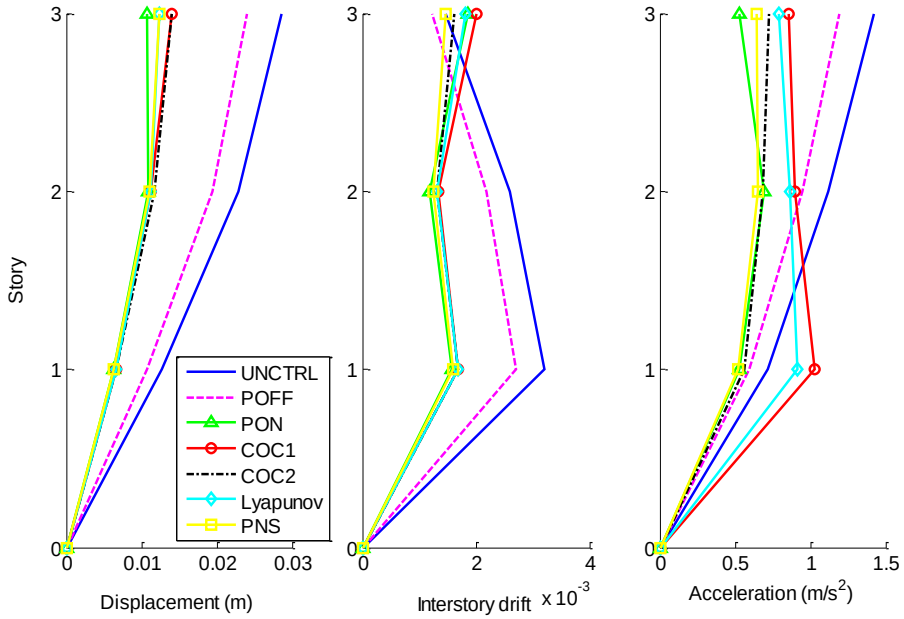

(b)

Figure 3: Uncontrolled and controlled responses under El Centro earthquake over the height of the adjacent buildings.
(a) RMS responses of building 1 (b) RMS responses of building 2

Controller	Evaluation Criteria										
	J1	J2	J3	J4	J5	J6	J7	J8	J9	J10	J11
PON	0.694	0.757	0.926	0.757	0.524	0.542	0.659	0.544	0.107	4778	908
COC1	0.648	0.788	0.932	0.799	0.451	0.490	0.725	0.493	0.117	5202	847
COC2	0.741	0.815	0.839	0.753	0.560	0.564	0.620	0.562	0.089	3945	684
Laypunov	0.812	0.722	0.895	0.726	0.622	0.664	0.807	0.665	0.110	4882	808
PNS	0.751	0.861	0.876	0.832	0.595	0.599	0.710	0.601	0.068	3035	668

Table 3: Comparison results under different control strategies for building 1 (9 stories).

Controller	Evaluation Criteria										
	J1	J2	J3	J4	J5	J6	J7	J8	J9	J10	J11
PON	0.475	0.773	0.519	0.588	0.379	0.581	0.489	0.493	0.333	4778	908
COC1	0.658	0.908	0.914	0.624	0.493	0.629	0.725	0.526	0.362	5202	847
COC2	0.588	0.686	0.617	0.573	0.492	0.526	0.512	0.528	0.275	3945	684
Laypunov	0.604	0.811	0.751	0.649	0.433	0.564	0.642	0.524	0.340	4882	808
PNS	0.497	0.604	0.501	0.604	0.435	0.497	0.457	0.499	0.211	3035	668

Table 4: Comparison results under different control strategies for building 2 (3 stories).

The results demonstrate that using MR damper as the coupling link is an effective way to reduce the responses of the adjacent buildings under earthquake input. Several observations are made. (i) The response mitigation is more obvious for shorter building. (ii) For taller building, COC1 provided the best control performance considering displacement, interstory drift and base shear. COC2 have the best performance in terms of acceleration. For shorter building, PON, COC2 and PNS control give similar results. Generally speaking, PON usually has slightly better control of peak displacement, while PNS performs slightly better in miti-

gating interstory drift and acceleration. (iii) In terms of the control force, the semi-active controllers always outperform the passive on case, especially for COC2 and PNS, with reduction around 25%.

3.2 Control performance assessment (nonlinear)

In this section, numerical simulation is conducted to evaluate the controller performance on a nonlinear model of the multi-story adjacent buildings system represented by hysteretic Bouc Wen model. The evaluation results of the control performance under El Centro earthquake using the proposed criteria are listed and compared in Tables 5 and 6. The uncontrolled and COC2 controlled time histories of the top floor responses for both buildings are given in Figure 4.

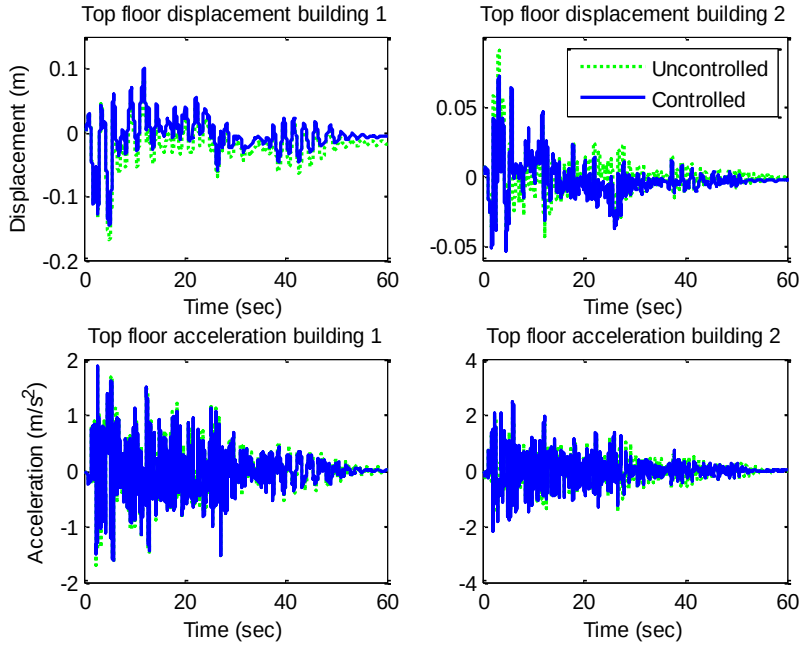

Figure 4: Time histories of top floor responses under COC2 control (nonlinear).

Controller	Evaluation Criteria										
	J1	J2	J3	J4	J5	J6	J7	J8	J9	J10	J11
PON	0.889	0.958	1.085	0.965	0.835	0.996	1.082	0.963	0.035	1559	399
COC1	0.773	0.902	1.095	0.978	0.805	0.921	1.074	0.932	0.027	1218	311
COC2	0.869	0.954	0.981	0.992	0.855	1.014	1.048	0.953	0.025	1100	231
Laypunov	0.882	1.023	0.953	1.002	0.840	1.015	1.087	0.978	0.037	1656	364
PNS	0.925	1.004	0.966	1.003	0.879	0.993	1.031	0.966	0.022	980	279

Table 5: Comparison results under different control strategies for building 1 (9 stories).

Controller	Evaluation Criteria										
	J1	J2	J3	J4	J5	J6	J7	J8	J9	J10	J11
PON	0.749	0.864	0.981	0.977	0.976	0.915	0.889	0.935	0.109	1559	399
COC1	0.806	0.792	1.178	0.964	1.136	0.951	1.005	0.899	0.085	1218	311
COC2	0.808	0.778	1.135	0.959	0.989	1.007	0.961	0.915	0.077	1100	231
Laypunov	0.888	0.949	1.318	1.012	1.042	0.932	0.953	0.924	0.115	1656	364

PNS	0.868	0.918	0.944	0.991	0.965	0.904	0.823	0.928	0.068	980	279

Table 6: Comparison results under different control strategies for building 2 (3 stories).

In general, the response reduction achieved in nonlinear cases is limited compare to the linear cases. The results follow the similar trends as the linear cases. Semi-active controller COC2 and PNS achieve the similar results using much less energy when comparing with PON. In Figure 4, it is observed that the residual displacements of both the buildings decrease compare to the uncontrolled case. The effectiveness of using MR damper as the coupling link to nonlinear adjacent structures is shown here.

3.3 Robustness analysis

The change of the dynamic properties of a building after strong earthquake due to the damage can be substantial. In order to include the stiffness degradation effects, a post-earthquake model (case 1) and a pre-earthquake model (case 3) are developed with 10% changes of the natural frequency from the nominal structural model (case 2). The robustness of different control algorithms are examined by the simulation using these models. The variation of control performance evaluated using index J5-J8 of the three cases are compared in Figures 5 and 6.

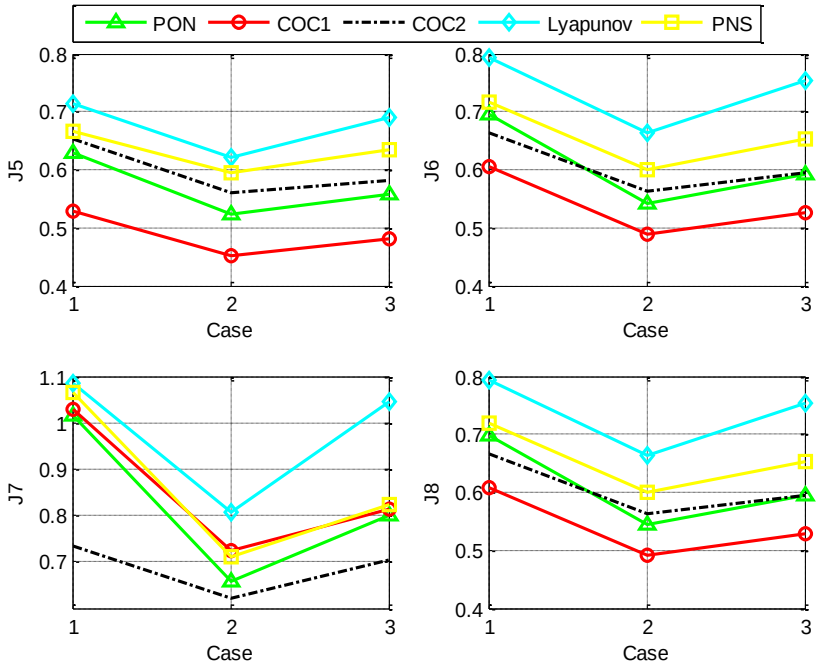

Figure 5: Variation of evaluation criteria indicators for building 1.

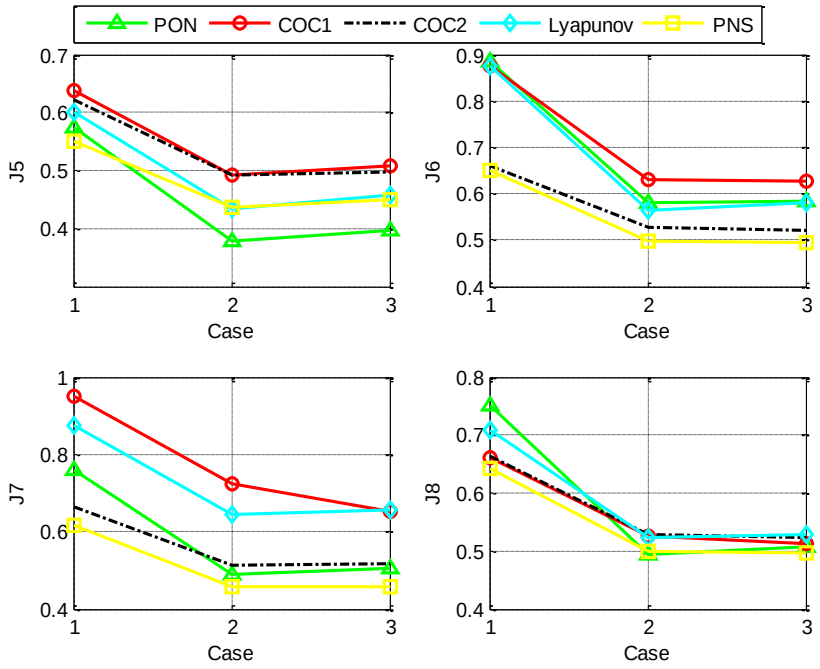

Figure 6: Variation of evaluation criteria indicators for building 2.

It is observed that, although the controllers are designed based on the nominal model, significant response mitigation is achieved for the post-earthquake and pre-earthquake cases as well, which confirms that the MR damper can provide reliable and robust control when the structure property changes. It is found that COC1 has better control considering displacement, interstory drift and base shear for building 1. PON provides a better control of displacement for building 2. COC2 and PNS are the most effective controllers in reducing interstory drift and acceleration of building 2.

The variation in the response using three models is less severe for COC2 in comparison to the other controllers of both buildings. Generally speaking, semi-active controller COC2 provides a more robust control. When facing changing conditions, the semi-active control system can still perform adequately and provide consistent levels of reduction.

4 CONCLUSIONS

The effectiveness in seismic response reduction of coupled building system interconnected by a MR damper is investigated for both linear and nonlinear cases. Different control strategies, including passive on, clipped optimal control, Lyapunov control and pseudo-negative stiffness (PNS) control are designed and evaluated. Some further robustness analyses are also performed. The following general conclusions can be drawn based on the simulation results:

- Using MR damper as the coupling link is effective in mitigating the dynamic responses of both of the adjacent buildings under earthquake input.
- For taller building, controller COC1 results in lower responses in terms of displacement, interstory drift and base shear. COC2 performs better in acceleration control. For shorter building, PON, COC2 and PNS control give very similar results. The response mitigation is relatively more obvious for shorter building.

- Semi-active controllers COC2 and PNS are superior at utilizing smaller damper force to achieve good control performance. 25% of energy can be saved compare to passive control.
- The residual displacements of both the buildings decrease in the nonlinear coupled building system with proper control.
- The robustness of semi-active controller COC2 is demonstrated through comparing the simulation results using pre-earthquake, nominal and post-earthquake models. Stable and robust control is still guaranteed by semi-active vibration control when the properties of the building changes.
- Generally speaking, semi-active controllers COC2 and PNS achieve better performance considering response reduction, robustness and energy saving. Moreover, semi-active controllers are more flexible compare to passive control, as the controller can be designed optimizing different control objectives.

REFERENCES

[1] R.E. Christenson, B.F. Spencer, E.A. Johnson, K. Seto, Coupled Building Control Considering the Effects of Building/Connector Configuration. *Journal of structural engineering ASCE*, **132**(6), 853-863, 2006.

[2] R.E. Christenson, B.F. Spencer, E.A. Johnson, Semiactive Connected Control Method for Adjacent Multidegree-of-Freedom Buildings. *Journal of Engineering Mechanics*, **133**, 290-298, 2007.

[3] HP. Zhu, H. Iemura, A study of response control on the passive coupling element between two parallel structures. *Structural Engineering and Mechanics*, **9**(4), 383-396, 2000.

[4] B.F. Spencer, S.J. Dyke, M.K. Sain, J.D. Carlson, Phenomenological model for magnetorheological dampers. *Journal of Engineering Mechanics,* **123**(3), 230-238, 1997.

[5] S.J. Dyke, B.F. Spencer, M.K. Sain, J.D. Carlson, Modeling and control of magnetorheological dampers for seismic response reduction. *Smart Materials & Structures*, **5**(5), 565-575, 1996.

[6] G. Leitmann, Semiactive Control for Vibration Attenuation. *Journal of Intelligent Material Systems and Structures*, **5**(6), 841-846, 1994.

[7] H. Iemura, A. Igarashi, N. Nakata, Semi-active control of full-scale structures using variable joint damper system. *Proceedings of the KKNN Symposium on Civil Engineering*, Kyoto, November 5-7, 41-46, 2001.

[8] H. Iemura, MH. Pradono, Passive and semi-active response control of a cable-stayed bridge. *Journal of Structural Control*, **9**, 189-204, 2002.

[9] H. Iemura, A. Igarashi, MH. Pradono, A. Kalantari, Negative stiffness friction damping for seismically isolated structures. *Journal of Structural Control and Health Monitoring*, **13**, 775-791, 2006.

[10] NEHRP Recommended Provisions for Seismic Regulations for New Buildings and Other Structures, *Report No. FEMA 450*, Washington, DC. , 2003.